

Temperature effects in articular cartilage biomechanics

Ronald K. June^{1,2,*} and David P. Fyhrie²

¹University of California, San Diego, Department of Cellular and Molecular Medicine, 9500 Gilman Drive, MC 0686, La Jolla, CA 92093-0686, USA and ²University of California, Davis, Departments of Orthopaedic Surgery and Biomedical Engineering, Sacramento, CA 95817, USA

*Author for correspondence (rkjune@gmail.com)

Accepted 5 August 2010

SUMMARY

Articular cartilage is the soft tissue that covers contacting surfaces of bones in synovial joints. Cartilage is composed of chondrocytes and an extracellular matrix containing numerous biopolymers, cations and water. Healthy cartilage functions biomechanically to provide smooth and stable joint movement. Degenerative joint diseases such as osteoarthritis involve cartilage deterioration, resulting in painful and cumbersome joint motion. Temperature is a fundamental quantity in mechanics, yet the effects of temperature on cartilage mechanical behavior are unknown. This study addressed the questions of whether cartilage stiffness and stress relaxation change with temperature. Samples of middle-zone bovine calf patellofemoral cartilage were tested in unconfined compression first at 24°C and then again after heating to 60°C. The data reveal that when temperature increases: (1) both peak and equilibrium stiffness increase by 150 and 8%, respectively, and (2) stress relaxation is faster at higher temperature, as shown by a 60% decrease in the time constant. The increases in temperature-dependent stiffness are consistent with polymeric mechanisms of matrix viscoelasticity but not with interstitial fluid flow. The changes in the time constant are consistent with a combination of both fluid flow and matrix viscoelasticity. Furthermore, we discovered a novel phenomenon: at stress-relaxation equilibrium, compressive stress increased with temperature. These data demonstrate a rich area of cartilage mechanics that has previously been unexplored and emphasize the role of polymer dynamics in cartilage viscoelasticity. Further studies of cartilage polymer dynamics may yield additional insight into mechanisms of cartilage material behavior that could improve treatments for cartilage degeneration.

Supplementary material available online at <http://jeb.biologists.org/cgi/content/full/213/22/3934/DC1>

Key words: cartilage, cartilage mechanics, osteoarthritis, flow-independent viscoelasticity, matrix viscoelasticity, polymer dynamics.

INTRODUCTION

Articular cartilage is the soft tissue that lines contacting surfaces of bones in synovial joints. Cartilage functions as a low-friction-bearing surface to enable smooth articulation during joint motion (Wright and Dowson, 1976). The primary components of articular cartilage are chondrocytes and a polymeric extracellular matrix consisting mainly of collagen, the proteoglycan aggregate, water and cations (Mow et al., 1992).

Previous studies have examined cartilage material properties in response to various experimental perturbations including enzymatic digestion (Basalo et al., 2005; Bonassar et al., 1995; DiSilvestro and Suh, 2002; Zhu et al., 1993) and ionic concentration (Dean et al., 2006; June et al., 2009; Lu et al., 2004). Static properties of articular cartilage result at least partially from electrostatic interactions between anionic glycosaminoglycans (Dean et al., 2006; Lu et al., 2004; Lux Lu et al., 2007).

Temperature is a fundamental quantity in mechanics (Holzapfel, 2000). However, the effects of temperature on cartilage material properties have not been studied. A complete understanding of cartilage mechanics requires an understanding of the effects of temperature on cartilage material properties. Hence, the first objective of this study was to determine whether cartilage mechanical properties change with temperature.

Cartilage viscoelasticity may originate from both flow-dependent and flow-independent mechanisms (Huang et al., 2001; Huang et al., 2003; Mow et al., 1980). Flow-dependent viscoelasticity results from interstitial fluid flow that is induced by pressure gradients that

develop upon tissue loading (Armstrong et al., 1984; Mow et al., 1980). Flow-independent viscoelasticity is thought to originate from the macromolecules of the cartilage extracellular matrix (Huang et al., 2001; Zhu et al., 1993).

Increased cartilage temperature may affect the behavior of both the interstitial water and the extracellular matrix. Fluid viscosity decreases with temperature (<http://webbook.nist.gov/chemistry/>). Stress relaxation of polymeric molecules such as those of the extracellular matrix is faster at higher temperatures (Doi and Edwards, 1988). Because cartilage is a fluid-filled polymeric solid, our second objective was to test the hypothesis that cartilage stress relaxation proceeds faster at higher temperatures.

Understanding the effects of temperature on cartilage stiffness provides an experiment to discriminate between fluid flow and polymeric matrix viscoelasticity. Because fluid viscosity decreases with temperature (<http://webbook.nist.gov/chemistry/>), fluid-flow theories predict a decrease in dynamic stiffness upon temperature increase (Armstrong et al., 1984; Mow et al., 1980). Conversely, polymer stiffness has been shown to increase with temperature (Sneppen and Zocchi, 2005). Therefore, determining how the stiffness of cartilage changes with temperature provides an experimental method for discriminating between flow-dependent and matrix mechanisms of cartilage viscoelasticity. Thus, the third objective of this study was to determine whether cartilage stiffness changes with temperature.

We tested the effects of temperature on the stress relaxation of bovine calf cartilage samples. Osteochondral explants were harvested from the patellofemoral groove, and middle-zone cartilage

samples were tested in unconfined compression. Samples were tested twice, either at different temperatures or at constant temperature to control for potential effects of repeated testing. The data clearly demonstrate temperature-dependent effects in cartilage material behavior that have not previously been identified. Stress relaxation proceeded faster at higher temperatures, which is consistent with a combination of changes in fluid viscosity and polymer motion. Both dynamic and equilibrium stiffness increased at higher temperatures, consistent with polymeric viscoelasticity and inconsistent with fluid-flow theories. These data demonstrate a rich area of cartilage mechanics that has not been previously studied. Future studies may utilize these phenomena to provide additional mechanistic insight into structure–function relationships for cartilage, which may prove useful for treating diseases of cartilage degeneration.

MATERIALS AND METHODS

Tissue harvest and culture

Stifle joints from 1- to 3-month-old bovine calves were obtained from a local slaughterhouse and cultured in serum-free DMEM/F12 (Invitrogen 11330032; Carlsbad, CA, USA). Medium was supplemented with 0.1% bovine serum albumin (BSA; w/v, Sigma A9418; St Louis, MO, USA), insulin-transferrin-selenium (1 mg ml^{-1} , 0.55 mg ml^{-1} and $0.67\text{ }\mu\text{g ml}^{-1}$, respectively; Invitrogen 41400045), L-ascorbic-acid-2-phosphate ($50\text{ }\mu\text{g ml}^{-1}$; Sigma A8960) and antibiotics (penicillin at 100 units ml^{-1} and streptomycin at $100\text{ }\mu\text{g ml}^{-1}$; Invitrogen 15140155). Cylindrical samples were aseptically harvested from a standardized location on the patellofemoral groove using a 5 mm cork borer, and immersed in culture medium. The samples were trimmed to a standardized height ($3.76\pm 0.03\text{ mm}$) by removing the superficial and deep zones using a custom-slicing device as described previously (Khalafi et al., 2007). Samples were rinsed three times with sterile medium, immersed in 4 ml of fresh medium in 12-well plates and maintained at 37°C in the presence of 5% CO_2 in an incubator (HeraCell 150; Thermo Scientific, Milford, MA, USA).

Mechanical testing

Stress-relaxation tests were performed in unconfined compression at 24 and 60°C using an Enduratec ELF 3200 loading system (Bose Electroforce, Eden Prairie, MN, USA). The $24\text{--}60^\circ\text{C}$ temperature range was the greatest possible for this system. This range was selected based on pilot experiments (supplementary material Fig. S1)

that found that the variability of cartilage stress-relaxation is much greater than any differences in mechanical properties between 32 and 42°C . Temperature was controlled by a custom-built bath capable of controlling the steady-state sample temperature to within 0.1°C (supplementary material Fig. S2). Samples were removed from tissue culture and their diameters were measured using digital calipers ($\pm 0.01\text{ mm}$, Absolute Digimatic; Mitutoyo, Kawasaki, Japan). Cartilage explants were then placed in the loading system, and a 12.5 kPa pre-stress (Wong et al., 2000) was applied at a displacement rate of $50\text{ }\mu\text{m s}^{-1}$. Immediately after the 12.5 kPa pre-stress was achieved, the loading chamber was filled with room-temperature ($20\text{--}22^\circ\text{C}$) culture medium and temperature control was initiated. The initial sample height was defined as the height at which the pre-stress was achieved.

After 10 min of pre-stress equilibration, a 5% nominal compression was applied at 10 mm s^{-1} and held for 10 min, after which the temperature was either ramped to 60°C to examine temperature-dependence or maintained constant at 24°C for control samples to examine the effects of repeated loading. After the first test, the platens were raised, and samples were allowed to recover without any applied deformation for 5 min, followed by the same stress-relaxation testing protocol (12.5 kPa pre-stress for 10 min, 5% nominal compression, and 10 min of relaxation; Fig. 1). After the 60°C test, the specimen bath was allowed to cool for 10 min. This procedure was carried out on cartilage explants from 22 independent joints, with $N=15$ samples for the temperature-change protocol and $N=7$ samples for the control protocol.

Force data were sampled at a rate of $180\text{ samples s}^{-1}$ for stress relaxation and 1 sample s^{-1} for heating and cooling. Apparent stresses were calculated by dividing the compressive force by the sample cross-sectional area, which was calculated from the measured diameter. The dynamic stiffness was calculated by dividing the peak stress by the nominal strain, and the equilibrium stress was calculated by dividing the equilibrium stress by the nominal strain.

We observed that the compressive stress increased with temperature, including a local maximum in the temperature–stress curve that occurred at $\sim 57^\circ\text{C}$ (Fig. 4). To examine this phenomenon further, we subjected additional samples ($N=8$) to the same temperature protocol while under low-stress cyclical loading. (Note that peak stresses reached almost 500 kPa in the stress-relaxation tests.) Dynamic sinusoidal compression was applied at 1 cycle s^{-1} using a different loading system capable of reaching 65°C . Samples

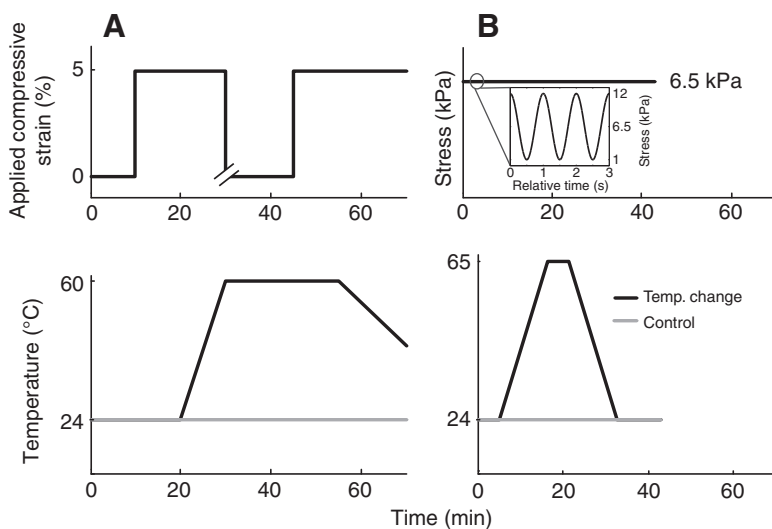


Fig. 1. Loading protocols used to investigate temperature in cartilage viscoelasticity. (A) Stress relaxation. Samples were equilibrated under 12.5 kPa pre-stress at 24°C and tested in stress relaxation at 5% unconfined compression followed by heating to 60°C , unloading and repetition of the stress-relaxation test. Subsequently, the samples were allowed to cool to 43°C . (B) Cyclical loading. Unconfined sinusoidal compression was applied at 1 Hz . Cyclical loading was load-controlled with a mean stress of 6.5 kPa and an amplitude of 5.5 kPa . The initial temperature was 24°C , after which temperature was ramped up to 65°C , held for 5 min, cooled to 24°C and held for 10 min. Control samples were tested at 24°C for both stress relaxation and cyclical loading.

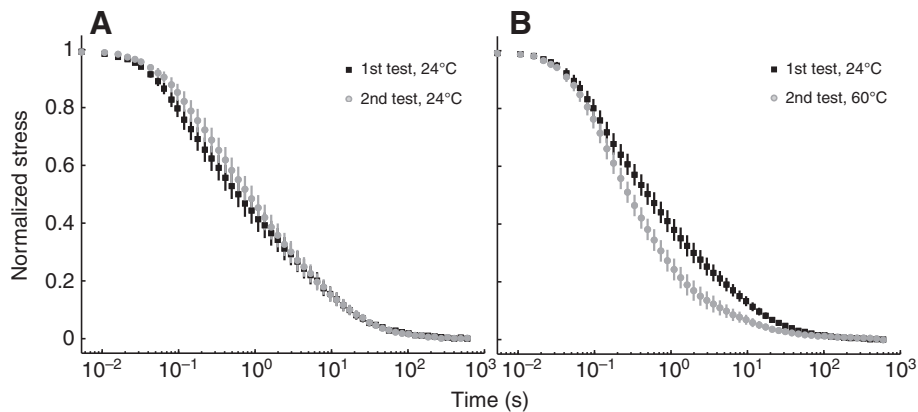


Fig. 2. Stress relaxation proceeds faster at 60°C than at 24°C. Stress-relaxation data were normalized to a range between one, representing the peak stress, and zero, representing the equilibrium stress. (A) Control samples were subjected to repeated stress-relaxation tests at a constant temperature. No statistically significant differences in any of the stretched exponential parameters were found between the first and second tests for the control samples. (B) Stress relaxation proceeded faster at 60°C than at 24°C. This accelerated stress relaxation may result from a combination of decreased fluid viscosity and faster polymer dynamics. Data are means \pm s.e.m.

were removed from culture, measured for height and diameter, and placed in a dynamic mechanical analyzer (DMA 7, Pyris Software Ver. 7.0.0.0110; Perkin Elmer, Waltham, MA, USA). The specimen bath was filled with medium, the temperature was set to 24°C and load-control sinusoidal loading was initiated at an average compressive stress of 6.5 kPa and an amplitude of 5.5 kPa. Samples were preconditioned at 24°C for 5 min, followed by a temperature increase to 65°C at a rate of 3.6°C min⁻¹ (the same heating rate as in the stress-relaxation experiments), held for 5 min and cooled to 24°C. The cyclical loading parameters (phase angle and storage modulus) were calculated using the proprietary software on the dynamic mechanical analyzer.

Analysis

Stress relaxation was quantified by two methods. First, data were normalized to a range between one, representing the peak stress, and zero, representing the equilibrium stress and plotted on a semilog scale. Second, stress-relaxation data were fitted with a stretched exponential model (Eqn 1) of stress relaxation, which has been used previously (June et al., 2009):

$$\sigma = (\sigma_{\text{peak}} - \sigma_{\text{eq}})e^{-(t/\tau)^\beta} + \sigma_{\text{eq}}, \quad (1)$$

where σ_{peak} and σ_{eq} are the peak and equilibrium stresses, respectively, which were defined by the experimental data; t is time; τ is the time constant; and β ($0 \leq \beta < 1$) is the stretching parameter with decreases in β representing increasingly heterogeneous relaxation dynamics (Lindsey and Patterson, 1980). τ and β were adjusted to fit the data using nonlinear minimization techniques (Boyd and Vandenberghe, 2004; June et al., 2009). The fitted model parameters were used to quantify differences in cartilage stress relaxation.

Statistical analysis was performed using repeated-measures ANOVA to compare each stress-relaxation parameter between control and treatment groups. Bonferroni *post hoc* tests were used to make comparisons between: (1) the first and second tests, and (2) treatment and control groups. Linear correlation between temperature and stress was used to assess temperature–stress relationships for the heating and cooling data. All data are expressed as means \pm s.e.m.

RESULTS

Increased temperature had marked effects on cartilage stress relaxation (Figs 2, 3, Table 1). Peak stress increased by 150% and equilibrium stress by 8% at 60°C compared with 24°C in the temperature-change group (both $P < 0.01$, $N = 15$). Stress relaxation proceeded faster with increased temperature as shown by the

normalized stress-relaxation data (Fig. 2) and the 60% decrease in the time constant τ ($P < 0.01$, $N = 15$). Both the dynamic and equilibrium stiffness increased with temperature (both $P < 0.01$, $N = 15$; Fig. 4). Increased temperature also resulted in a decrease in the stretching parameter, β , from 0.43 at 24°C to 0.33 at 60°C ($P < 0.01$, $N = 15$). No statistically significant differences were found in any stress-relaxation parameters for control samples subjected to repeated tests at the same concentration.

We found novel temperature-dependent behavior in cartilage: during heating, the compressive stress increased with increasing temperature and, during cooling, the stress decreased with decreasing temperature (Table 2, Fig. 5). The temperature dependence of the equilibrium stress was 77% greater for cooling (0.78 ± 0.07 kPa °C⁻¹) than for heating (0.44 ± 0.07 kPa °C⁻¹, $P < 0.01$, $N = 15$; Table 2). During the heating phase, a peak in the temperature–stress curve was observed at 57 ± 0.1 °C (Fig. 5). Cyclical loading under lower stresses (mean compressive stress of 6.5 kPa) revealed a temperature transition at 64 ± 0.3 °C, demonstrated by a phase lag peak (Fig. 6).

Linear regression on the last 2 s of the stress-relaxation data found no statistically significant slopes in any data set at the 99% confidence level, demonstrating that 10 min of stress relaxation were sufficiently long to produce an equilibrium to the applied 5% compression. To assess the unloaded recovery period between stress-relaxation tests, we performed linear regression of the final 2 s of preload stress-time data for the second stress-relaxation test. No significant slopes were found in any data set at the 99% confidence level, demonstrating that the recovery period between tests was sufficient. Furthermore, the difference between sample heights at 24 and 60°C was not statistically significant ($P = 0.37$).

DISCUSSION

Cartilage is a complex tissue containing a heterogeneous three-dimensional extracellular matrix composed of multiple biopolymers, cations and water. The *in vivo* function of cartilage is primarily mechanical: to provide a smooth surface for joint articulation. Because cartilage function is mechanical, understanding the mechanical properties of cartilage is necessary to understand cartilage function. As such, the objectives of this study were to: (1) determine whether the mechanical properties of cartilage changed with temperature, and test the hypotheses that (2) cartilage stress relaxation is faster at higher temperature and (3) cartilage stiffness increases with temperature.

We found that stress relaxation was markedly different between 24 and 60°C. Furthermore, we discovered novel cartilage behavior: at 5% stress-relaxation equilibrium, compressive stress was proportional to temperature. The stress-relaxation testing protocol

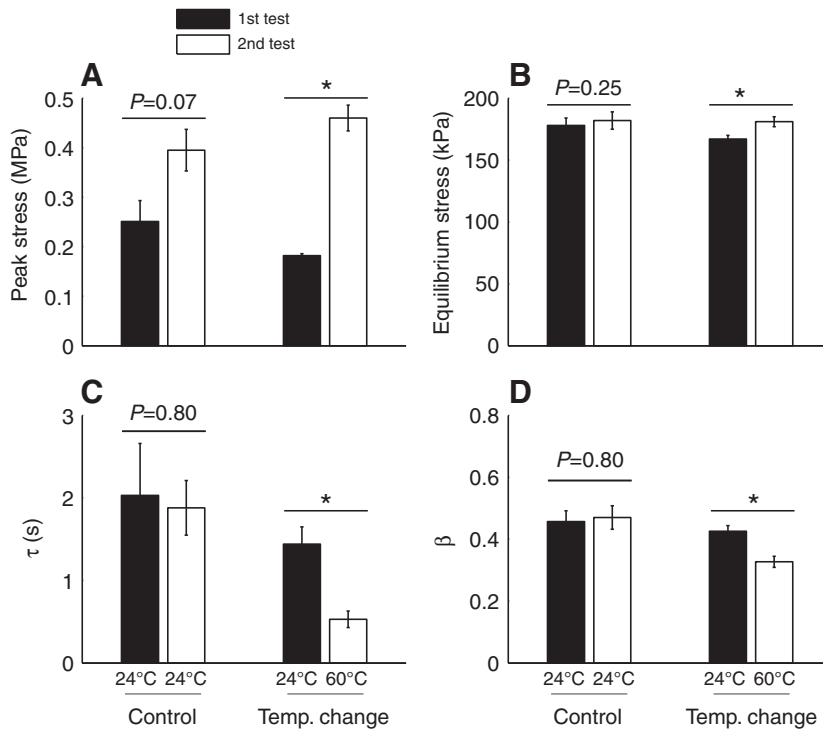


Fig. 3. Stretched exponential model finds temperature-dependent changes in stress-relaxation: higher peak and equilibrium stresses and faster dynamics at 60°C than at 24°C. Asterisk indicates $P < 0.01$ for Bonferroni *post hoc* test ($N=8$ for control and 15 for temperature change). (A) Samples tested at 60°C exhibited a larger peak stress than samples tested at 24°C. The peak stress change for the control samples was not statistically significant ($P=0.07$). (B) Increased temperature resulted in a larger equilibrium stress. (C) The time constant (τ) decreased markedly at high temperature. (D) The stretching parameter (β) decreased upon temperature increase. Data are means + s.e.m.

applied a 5% nominal compression in less than 20 ms whereas previous experiments have used loading times ranging from ~1 (Huang et al., 2003) to 500 s (Basalo et al., 2004; Park et al., 2003). Our rapid load application revealed fast relaxation dynamics that have not previously been emphasized: about 80% of the stress-relaxation occurred during the first 100 s (Fig. 2). These data add a novel experimental phenomenon to an already complex picture of cartilage mechanics (Dean et al., 2006; Federico et al., 2005; Julkunen et al., 2008; Neu et al., 2007; Park et al., 2003).

Cartilage stress relaxation was faster at 60°C than at 24°C, as shown by both the normalized stress-relaxation data (Fig. 2) and the 60% decrease in τ . Neither of the putative mechanisms of cartilage viscoelasticity (flow-dependent or flow-independent) can solely explain this observation. However, the combination of flow-dependent and flow-independent mechanisms does explain the data. Between 24 and 60°C, the viscosity of water decreases by 49% (<http://webbook.nist.gov/chemistry/>). Thus, faster fluid flow would predict a 49% decrease in τ , assuming a linear relationship between the stress-relaxation time constant and water viscosity. The remaining decrease in τ may result from changes in the dynamics of the extracellular matrix biopolymers, which are predicted to be inversely proportional to the change in absolute temperature (Doi, 1995; Doi and Edwards, 1988). Absolute temperature increased by 12% in our experiments. The combination of a decrease in viscosity

(49%) and an increase in polymer motion (12%) may explain the total observed decrease in τ (60%). Individually, neither mechanism can explain the experimentally observed changes; only the combination of flow-dependent viscosity decrease and flow-independent polymer motion explains the data.

By mass, cartilage is ~60–80% water, 10–20% collagen and 4–7% proteoglycan aggregate (Mankin et al., 2000). The interactions between these components are paramount to tissue function. For example, in cartilage the proteoglycan aggregate is compressed to a small fraction of its free-swelling volume (Kuettner and Kimura, 1985). Additionally, water in cartilage can be separated into fibrillar and intrafibrillar compartments (Wachtel and Maroudas, 1998). The physics of polymers such as those of the cartilage extracellular matrix is strongly dependent on interactions with the solvent, which in cartilage is assumed to be water (Doi and Edwards, 1988). Despite these complexities, the correlation between the experimental data (60% change in τ) and the combined theoretically predicted changes in dynamics (49% change in water viscosity and 12% change in polymer motion) is remarkable.

Both the dynamic and equilibrium stiffnesses of cartilage increased with temperature. Because fluid viscosity decreases with temperature, the increases in stiffness cannot represent a flow-dependent phenomenon. Polymer stiffness is known to increase with temperature (Sneppen and Zocci, 2005), and the solid matrix of

Table 1. Stress relaxation proceeded faster in the 60°C samples than in the 24°C samples, as shown by differences in both the stretched exponential time constant (τ) and the stretching parameter (β)

	Test	Peak stress (kPa)	Equilibrium stress (kPa)	τ (s)	β
Control	1st (24°C)	251±42	178±6	2.03±0.63	0.457±0.035
	2nd (24°C)	395±42	182±7	1.88±0.33	0.470±0.038
Temp. change	1st (24°C)	182±4*	167±3*	1.44±0.21*	0.426±0.018*
	2nd (60°C)	460±26	181±4	0.53±0.10	0.327±0.018

The peak stress change for the control samples was not statistically significant ($P=0.07$). *, $P < 0.01$ ($N=8$ for control and 15 for temperature change) for paired comparison between the 1st and 2nd tests within a group using Bonferroni *post hoc* tests.

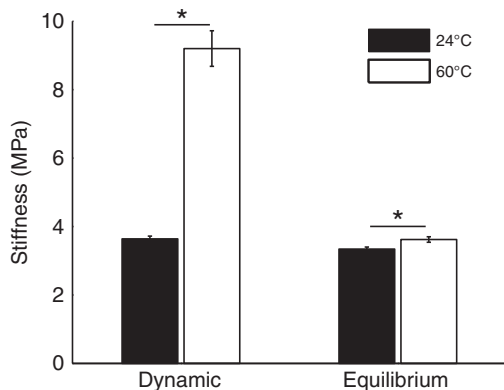


Fig. 4. Cartilage stiffness increases with temperature. Asterisk indicates $P < 0.01$ for Bonferroni *post hoc* test ($N=15$). Both the dynamic (left) and equilibrium (right) stiffness were greater at 60°C (white bars) than at 24°C (black bars). Stiffness was calculated by dividing the measured stress by the nominal strain.

articular cartilage is mainly composed of biopolymers. The reason for the temperature-induced stiffening of polymers is that the end-to-end distribution of polymer lengths is primarily driven by entropy, which increases with temperature. The temperature-induced increases in stiffness are probably caused by increases in the stiffness of the extracellular matrix biopolymers, consistent with previously developed theoretical models of cartilage (Kovach, 1995; Kovach, 1996).

At stress-relaxation equilibrium, compressive stress increased with temperature by a mean of 8% between 24 and 60°C. Between these temperatures, the specific volume of water increases by only 1.4% (<http://webbook.nist.gov/chemistry/>), so the expansion of water might have minimally contributed to the temperature-dependent increase in equilibrium stress. Polymers such as those of the cartilage matrix are known to swell with temperature (Doi, 1995), and expansion of the polymeric extracellular matrix might also have contributed to the temperature-dependent increase in equilibrium stress.

Cyclical loading revealed a phase-lag peak that is indicative of a temperature transition at 64°C, which is consistent with previous research on collagen thermodynamics. Previous research on the thermodynamics of solution-phase type I collagen has found that, upon heating, crystalline regions melt at 64°C (Flory and Garrett, 1958). Although cartilage contains mostly type II collagen, the collagens are highly conserved proteins – bovine types I and II have substantial sequence homology (supplementary material Fig. S4) – justifying comparison between the two types.

Table 2. Stress increased with increasing temperature and decreased with decreasing temperature, with strong linear associations

	Slope (kPa °C ⁻¹)	r
Heating	0.44±0.07	0.96±0.01
Cooling	0.78±0.07	0.96±0.03

The slope for cooling was significantly higher than the slope for heating ($P < 0.01$, $N=15$), consistent with a melting of regions of crystalline collagen [represented by the peak in the stress-temperature curve (Fig. 4) and the cyclical loading transition (Fig. 5)], which allows greater mobility of cartilage polymers, manifested in the greater dependence of equilibrium stress on temperature.

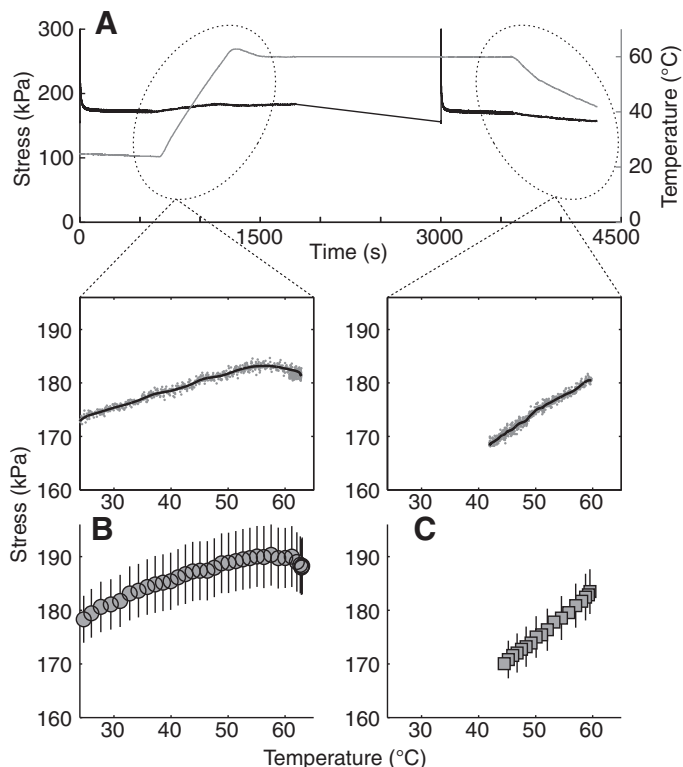


Fig. 5. Novel temperature-dependent increases in equilibrium stress.

(A) Representative set of experimental data. Top: stress and temperature as a function of time; bottom: temperature *versus* stress for the indicated heating and cooling regions. The black line is a 25-point moving average. (B) Average heating data. Equilibrium stress increased with increasing temperature (stress-temperature slope: 0.44 ± 0.07 kPa °C⁻¹, $r = 0.96 \pm 0.01$). There was a local maximum in the stress-temperature data at 57 ± 0.77 °C. This was likely due to melting of a crystalline collagen region (Flory and Garrett, 1957), which may occur at a lower temperature in these experiments owing to the strain energy resulting from the 5% compression applied prior to heating. (C) Average cooling data. Equilibrium stress decreased with decreasing temperature upon cooling (slope: 0.78 ± 0.07 kPa °C⁻¹, $r = 0.96 \pm 0.03$). Data in B and C are means \pm s.e.m.

The 64°C transition observed in these cyclical loading experiments probably represents melting of crystalline regions of collagen, which has previously been found at 63–64°C in type I collagen (Flory and Garrett, 1958). The 57°C local maximum in the stress-temperature heating data may also result from melting of crystalline collagen, albeit at a lower temperature owing to the additional strain energy resulting from the 5% compression. This interpretation is supported by our observation that the stress-temperature dependence (Table 2) is stronger for cooling (after the melting would have happened) than for heating (while the crystalline regions may have been intact); melted regions will have higher mobility than crystalline regions, resulting in faster molecular motion to relieve the stress associated with the applied compression.

In the stress-relaxation experiments, the decrease in β demonstrates increasing heterogeneity of the relaxation processes with increased temperature (Lindsey and Patterson, 1980). This is consistent with collagen melting: the melted crystalline regions of collagen will exhibit distinct dynamics, which may partially explain the decreases in β . Melted crystalline regions of collagen may also enable altered dynamics within the noncollagenous components of

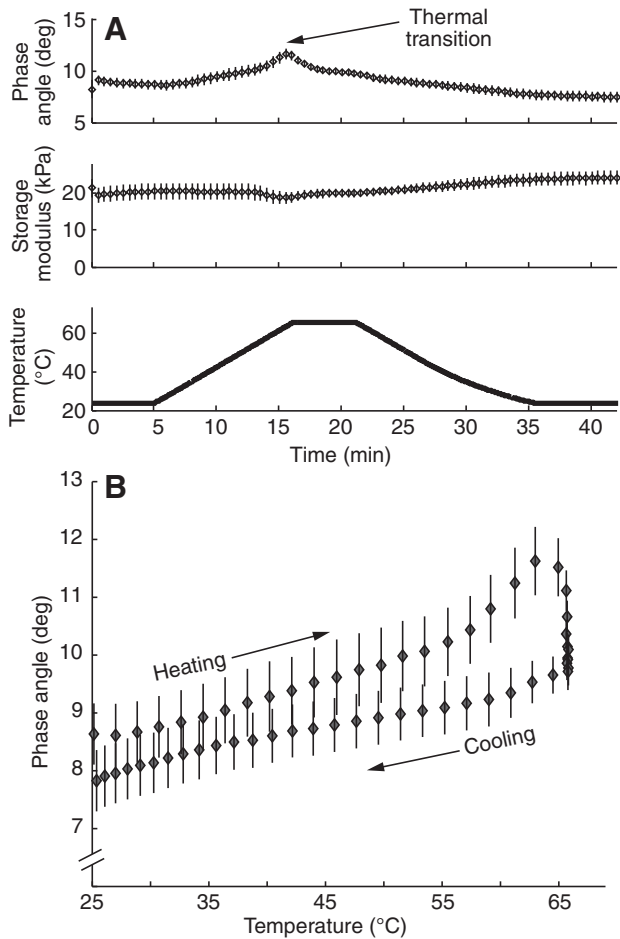


Fig. 6. Thermal transition at 64°C in cartilage samples subjected to sinusoidal unconfined compression. (A) Data plotted versus time. (B) Phase angle data plotted as a function of temperature. 1 Hz cyclical loading at a mean stress of 6.5 kPa revealed a phase angle peak at 64°C. Previous research (Flory and Garret, 1958) has found that crystalline regions of collagen melt at this temperature. Melting of regions of collagen crystallinity may explain the peak in the stress–temperature data from the stress–relaxation experiments, which could occur at a lower temperature (57°C) because of the strain energy associated with the 5% compression. Data are means \pm s.e.m.

cartilage (e.g. water and the proteoglycan aggregate may behave differently), which may also explain the decreases in β .

When considering these data, some limitations should be noted. First, we used cartilage explants maintained in tissue culture, and the temperature increase may have affected chondrocyte biology (e.g. by inducing the release of proteolytic enzymes). It is unknown whether altered chondrocyte biology could have substantially altered cartilage material properties during the time scale of this experiment (~60 min). However, the half-lives of collagen and aggrecan are on the order of years (Maroudas et al., 1998; Maroudas et al., 1992; Verzijl et al., 2000), suggesting that substantial induced proteolysis would be needed to induce major changes in these matrix molecules during the relatively short experimental time course. Additionally, the maximum temperature used in this study was well above physiological temperature. Despite this limitation, we believe that the resulting data provide an improved picture of cartilage mechanics. Understanding the dynamics of the matrix biopolymers may yield important insight for novel therapeutic targets and

strategies for the treatment and/or prevention of osteoarthritis. Future studies may provide further insight into the nature of cartilage mechanics by using the temperature-dependent behavior discovered in this study.

SUMMARY

We determined the mechanical properties of articular cartilage explants at different temperatures. Stress relaxation was faster at higher temperatures, consistent with a combination of changes in fluid viscosity and extracellular matrix polymer dynamics. Both the dynamic and equilibrium stiffness increased with temperature, consistent with polymer mechanisms. Novel temperature-dependent increases in equilibrium stress were observed and may result from the swelling of water and matrix polymers. These data clearly demonstrate the presence of temperature-dependent effects in cartilage mechanics. Future studies may utilize these effects toward a better understanding of structure–function relationships in cartilage mechanics.

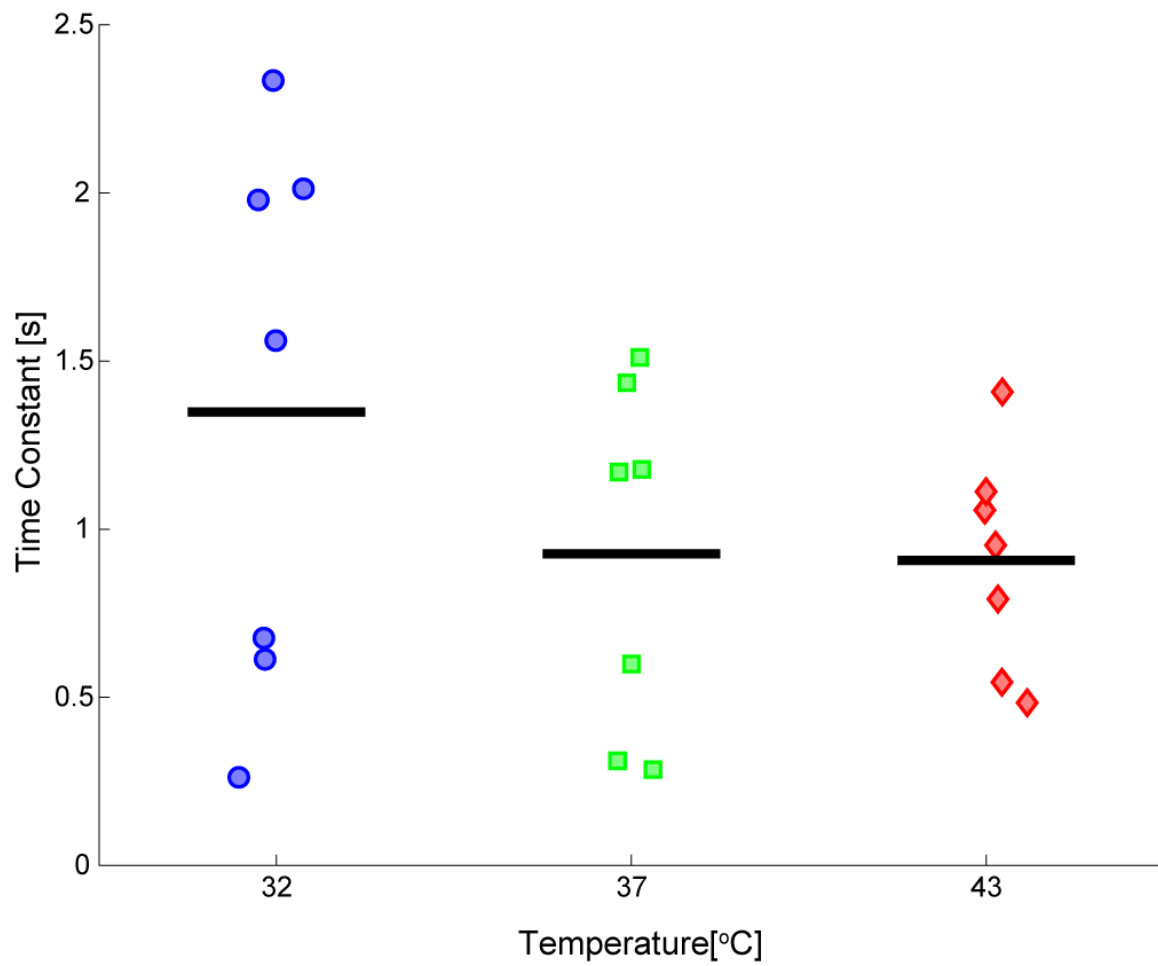
ACKNOWLEDGEMENTS

We gratefully acknowledge Professor A. H. Reddi for providing the cartilage samples. We thank Professor T. L. Kuhl and Dr G. S. Shapiro for helpful comments on the manuscript. We thank the David Linn Chair and NIH 5F31AR05086 for funding. Deposited in PMC for release after 12 months.

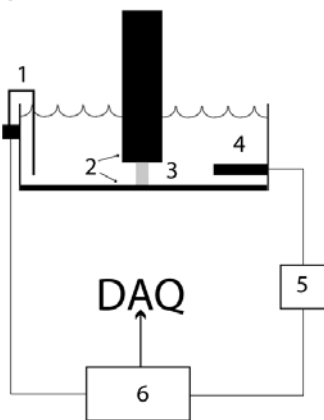
REFERENCES

- Armstrong, C. G., Lai, W. M. and Mow, V. C. (1984). An analysis of the unconfined compression of articular cartilage. *J. Biomech. Eng.* **106**, 165–173.
- Basalo, I. M., Mauck, R. L., Kelly, T. A., Nicoll, S. B., Chen, F. H., Hung, C. T. and Ateshian, G. A. (2004). Cartilage interstitial fluid load support in unconfined compression following enzymatic digestion. *J. Biomech. Eng.* **126**, 779–786.
- Basalo, I. M., Raj, D., Krishnan, R., Chen, F. H., Hung, C. T. and Ateshian, G. A. (2005). Effects of enzymatic degradation on the frictional response of articular cartilage in stress relaxation. *J. Biomech.* **38**, 1343–1349.
- Bonassar, L. J., Frank, E. H., Murray, J. C., Pagnolo, C. G., Moore, V. L., Lark, M. W., Sandy, J. D., Wu, J. J., Eyre, D. R. and Grodzinsky, A. J. (1995). Changes in cartilage composition and physical properties due to stromelysin degradation. *Arthritis Rheum.* **38**, 173–183.
- Boyd, S. and Vandenberghe, L. (2004). *Convex Optimization*. Cambridge, UK: Cambridge University Press.
- Dean, D., Han, L., Grodzinsky, A. J. and Ortiz, C. (2006). Compressive nanomechanics of opposing aggrecan macromolecules. *J. Biomech.* **39**, 2555–2565.
- DiSilvestro, M. R. and Suh, J. K. (2002). Biphasic poroviscoelastic characteristics of proteoglycan-depleted articular cartilage: simulation of degeneration. *Ann. Biomed. Eng.* **30**, 792–800.
- Doi, M. (1995). *An Introduction to Polymer Physics*. Oxford, UK: Oxford University Press.
- Doi, M. and Edwards, S. F. (1988). *The Theory of Polymer Dynamics*. Oxford, UK: Oxford University Press.
- Federico, S., Grillo, A., La Rosa, G., Giaquinta, G. and Herzog, W. (2005). A transversely isotropic, transversely homogeneous microstructural-statistical model of articular cartilage. *J. Biomech.* **38**, 2008–2018.
- Flory, P. J. and Garrett, R. R. (1958). Phase transitions in collagen and gelatin systems. *J. Am. Chem. Soc.* **80**, 4836–4845.
- Holzappel, G. A. (2000). *Nonlinear Solid Mechanics: a Continuum Approach*. West Sussex: Wiley.
- Huang, C. Y., Mow, V. C. and Ateshian, G. A. (2001). The role of flow-independent viscoelasticity in the biphasic tensile and compressive responses of articular cartilage. *J. Biomech. Eng.* **123**, 410–417.
- Huang, C. Y., Soltz, M. A., Kopacz, M., Mow, V. C. and Ateshian, G. A. (2003). Experimental verification of the roles of intrinsic matrix viscoelasticity and tension-compression nonlinearity in the biphasic response of cartilage. *J. Biomech. Eng.* **125**, 84–93.
- Julkunen, P., Wilson, W., Jurvelin, J. S., Rieppo, J., Qu, C. J., Lammi, M. J. and Korhonen, R. K. (2008). Stress-relaxation of human patellar articular cartilage in unconfined compression: prediction of mechanical response by tissue composition and structure. *J. Biomech.* **41**, 1978–1986.
- June, R. K., Mejia, K. L., Barone, J. R. and Fyhrle, D. P. (2009). Cartilage stress-relaxation is affected by both the charge concentration and valence of solution cations. *Osteoarthr. Cartil.* **17**, 669–676.
- Khalafi, A., Schmid, T. M., Neu, C. and Reddi, A. H. (2007). Increased accumulation of superficial zone protein (SZP) in articular cartilage in response to bone morphogenetic protein-7 and growth factors. *J. Orthop. Res.* **25**, 293–303.
- Kovach, I. S. (1995). The importance of polysaccharide configurational entropy in determining the osmotic swelling pressure of concentrated proteoglycan solution and the bulk compressive modulus of articular cartilage. *Biophys. Chem.* **53**, 181–187.
- Kovach, I. S. (1996). A molecular theory of cartilage viscoelasticity. *Biophys. Chem.* **59**, 61–73.
- Kuettner, K. E. and Kimura, J. H. (1985). Proteoglycans: an overview. *J. Cell. Biochem.* **27**, 327–336.

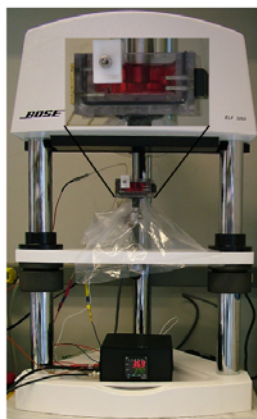
- Lindsey, C. and Patterson, G.** (1980). Detailed comparison of the Williams-Watts and Cole-Davidson functions. *J. Chem. Phys.* **73**, 3348-3357.
- Lu, X. L., Sun, D. D., Guo, X. E., Chen, F. H., Lai, W. M. and Mow, V. C.** (2004). Indentation determined mechano-electrochemical properties and fixed charge density of articular cartilage. *Ann. Biomed. Eng.* **32**, 370-379.
- Lux Lu, X., Miller, C., Chen, F. H., Edward Guo, X. and Mow, V. C.** (2007). The generalized triphasic correspondence principle for simultaneous determination of the mechanical properties and proteoglycan content of articular cartilage by indentation. *J. Biomech.* **40**, 2434-2441.
- Mankin, H. J., Mow, V. C., Buckwalter, J. A., Iannotti, J. P. and Ratcliffe, A.** (2000). Articular cartilage structure, composition, and function. In *Orthopaedic Basic Science: Biology and Biomechanics of the Musculoskeletal System* (ed. J. A. Buckwalter, T. A. Einhorn and S. R. Simon), pp. 443-470. Rosemont, IL: American Academy of Orthopaedic Surgeons.
- Maroudas, A., Palla, G. and Gilav, E.** (1992). Racemization of aspartic acid in human articular cartilage. *Connect. Tissue Res.* **28**, 161-169.
- Maroudas, A., Bayliss, M. T., Uchitel-Kaushansky, N., Schneiderman, R. and Gilav, E.** (1998). Aggrecan turnover in human articular cartilage: use of aspartic acid racemization as a marker of molecular age. *Arch. Biochem. Biophys.* **350**, 61-71.
- Mow, V. C., Kuei, S. C., Lai, W. M. and Armstrong, C. G.** (1980). Biphasic creep and stress relaxation of articular cartilage in compression: theory and experiments. *J. Biomech. Eng.* **102**, 73-84.
- Mow, V. C., Ratcliffe, A. and Poole, A. R.** (1992). Cartilage and diarthrodial joints as paradigms for hierarchical materials and structures. *Biomaterials* **13**, 67-97.
- Neu, C. P., Khalafi, A., Komvopoulos, K., Schmid, T. M. and Reddi, A. H.** (2007). Mechano-transduction of bovine articular cartilage superficial zone protein by transforming growth factor beta signaling. *Arthritis Rheum.* **56**, 3706-3714.
- Park, S., Krishnan, R., Nicoll, S. B. and Ateshian, G. A.** (2003). Cartilage interstitial fluid load support in unconfined compression. *J. Biomech.* **36**, 1785-1796.
- Sneppen, K. and Zocchi, G.** (2005). *Physics in Molecular Biology*. Cambridge, UK: Cambridge University Press.
- Verzijl, N., DeGroot, J., Thorpe, S. R., Bank, R. A., Shaw, J. N., Lyons, T. J., Bijlsma, J. W., Lafeber, F. P., Baynes, J. W. and TeKoppele, J. M.** (2000). Effect of collagen turnover on the accumulation of advanced glycation end products. *J. Biol. Chem.* **275**, 39027-39031.
- Wachtel, E. and Maroudas, A.** (1998). The effects of pH and ionic strength on intrafibrillar hydration in articular cartilage. *Biochim. Biophys. Acta* **1381**, 37-48.
- Wong, M., Ponticello, M., Kovanen, V. and Jurvelin, J. S.** (2000). Volumetric changes of articular cartilage during stress relaxation in unconfined compression. *J. Biomech.* **33**, 1049-1054.
- Wright, V. and Dowson, D.** (1976). Lubrication and cartilage. *J. Anat.* **121**, 107-118.
- Zhu, W., Mow, V. C., Koob, T. J. and Eyre, D. R.** (1993). Viscoelastic shear properties of articular cartilage and the effects of glycosidase treatments. *J. Orthop. Res.* **11**, 771-781.



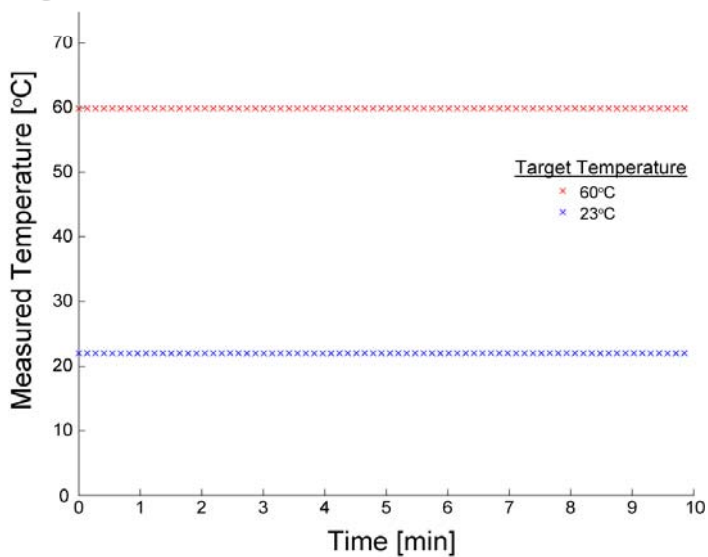
A

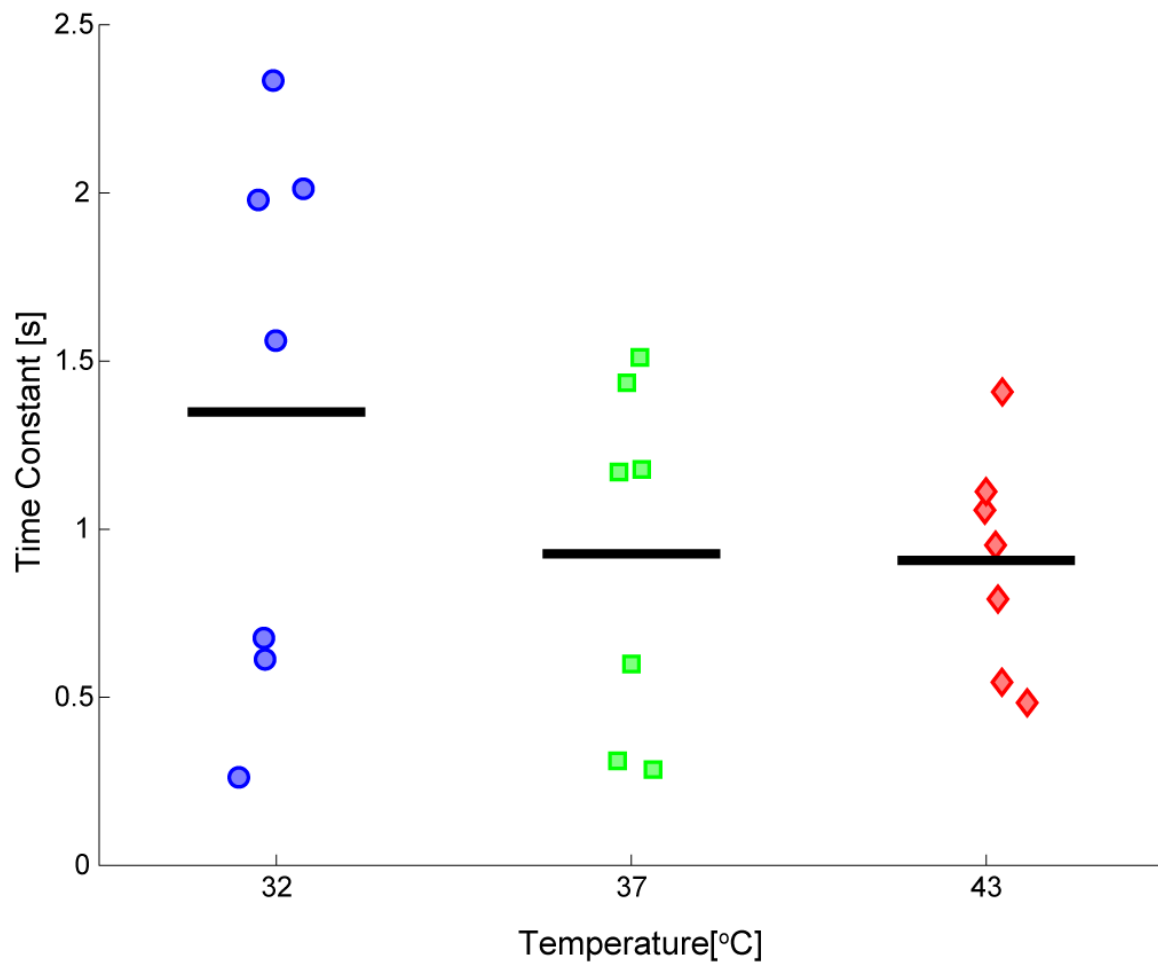


B

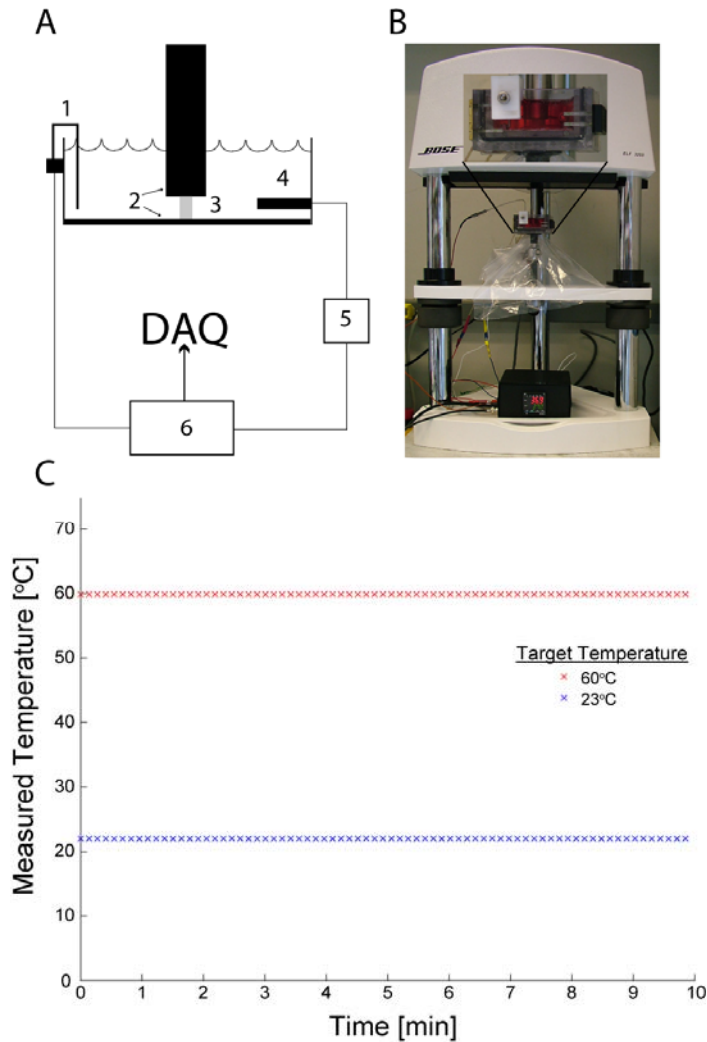


C

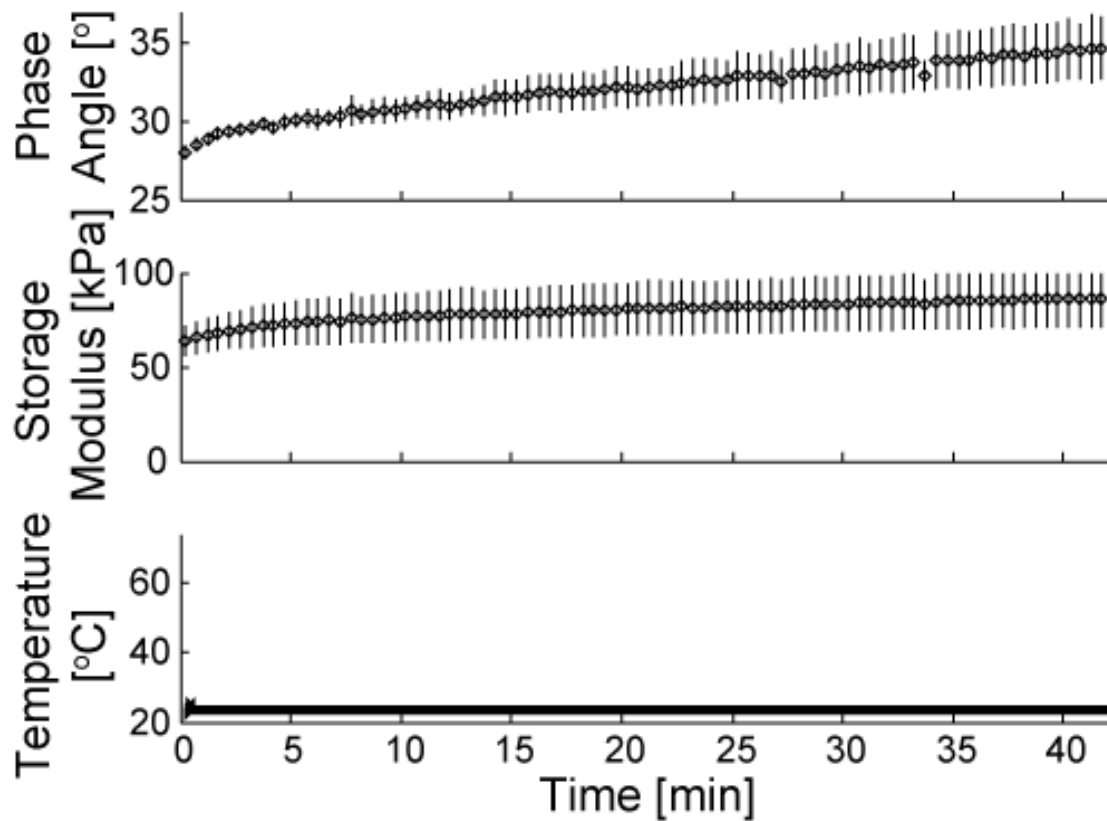




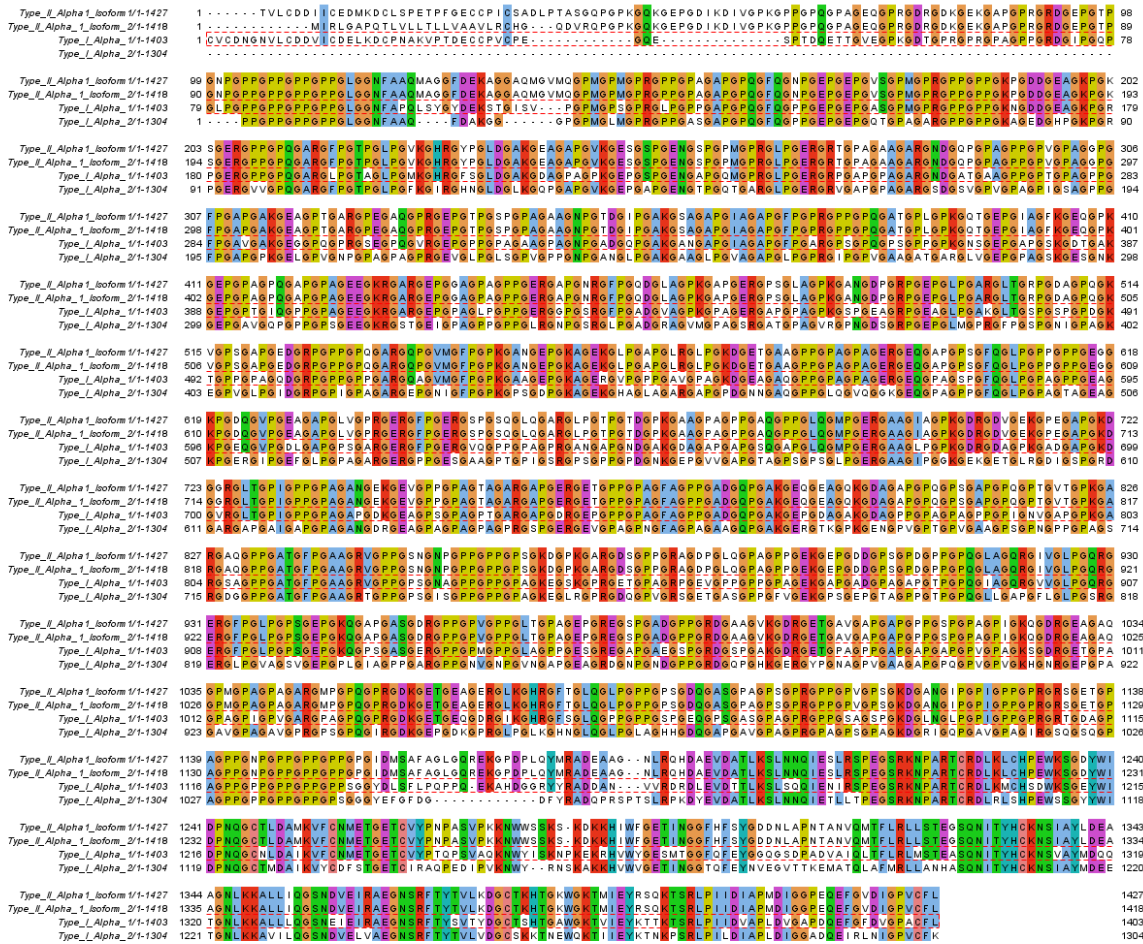
Supplementary Figure 2



Temperature Control System. (A) Schematic of loading system with temperature control. 1. thermocouple 2. polished stainless steel compression platens 3. cartilage sample 4. immersion heater 5. solid state relay 6. temperature controller. (B) Photograph of loading system with temperature control. (C) Validation data. The specimen bath was filled with media, and the temperature was ramped to either 23°C or 60°C. Data were collected at steady-state temperature. The standard deviation of the temperature measurements was 0.0070 at 23°C and 0.0069 at 60°C. These standard deviations are smaller than the bitwise resolution (0.01°C) of the temperature controller. At steady state, the thermocouple was manually placed at multiple positions within the bath, and the temperature was found to be spatially-homogeneous (data not shown). During the heating phase between stress-relaxation tests, the temperature reached a peak of $63.1 \pm 0.1^\circ\text{C}$ but dropped to a final steady-state value of $60.1 \pm 0.1^\circ\text{C}$ by the beginning of the second stress-relaxation experiment.



Supplemental Figure 4



Substantial protein homology between bovine type I and type II collagen chains. The amino acid sequences of all known bovine type I and II collagen alpha chains (type I: $\alpha 1$ NP_001029211, $\alpha 2$ NP_776945. Type II, $\alpha 1$: Isoform 1 NP_001001135, Isoform 2 NP_001106695) were aligned using ClustalW¹ and visualized using Jalview.² Residues are highlighted when 3 or more are identical in the multiple alignment. Pairwise alignments using BLAST found amino acid identity of 69 and 73% between the $\alpha 1$ chain of type I collagen and isoforms 1 and 2 of the type II chain, respectively. Pairwise alignments using BLAST found amino acid identity of 64% between the $\alpha 2$ chain of type I collagen and both isoforms 1 and 2 of the type II chain, respectively.

¹ MA Larkin *et al*, *Bioinformatics* 2007.
² AM Waterhouse *et al*, *Bioinformatics* 2009.

